

THEORY OF CUMULATIVE BEAM-BREAKUP WITH BNS DAMPING

K.Y. Ng and C.L. Bohn, FNAL,* Batavia, IL60510, USA

Abstract

Analytic tools for the study of multibunch cumulative beam breakup (MBBU) in linear colliders (LCs) including BNS damping are developed. One approach is to consider cases for which exponential growth of MBBU is noticeable, although one generally wishes to avoid this regime in LCs to make operations easier. By developing scaling relations, one is able to see at once how to suppress it effectively. The formalism to study MBBU including some interesting subtleties, such as BNS damping and misaligned accelerator components, is applied to both normal-conducting and superconducting linacs comprising LCs.

1 BEAM-BREAKUP EQUATION

One of the limitations of future LCs is the MBBU of a long bunch train driven by the transverse wake potential in the cavities of the linacs, especially when the size of the cavities is small. Other factors, such as cavity misalignments and focusing quadrupole offsets, will also contribute to the emittance increase of the beam and can result in beam loss as well as reduction in collision luminosity. A spread in the focusing strength of the quadrupoles, or equivalently a spread in energy, along the bunch train can provide BNS damping [1] that may keep emittance growth under control.

Consider a relativistic particle beam injected into a linac of length ℓ . At a distance $s = \sigma\ell$ into the linac, the transverse displacement $x(\sigma, \zeta)$ given beam energy $\gamma(\sigma)E_0$ with E_0 the rest energy satisfies the differential equation

$$\frac{1}{\gamma(\sigma)} \frac{\partial}{\partial \sigma} \left[\gamma(\sigma) \frac{\partial x(\sigma, \zeta)}{\partial \sigma} \right] + \kappa^2(\sigma, \zeta) [x(\sigma, \zeta) - x_Q(\sigma)] = \epsilon \int_0^\zeta d\zeta' w(\zeta - \zeta') F(\zeta') [x(\sigma, \zeta') - x_A(\sigma)], \quad (1)$$

where $\zeta/\omega_r = t - s/c$, with c the velocity of light, is the time measured after the arrival of the first bunch at position σ . Here, ω_r is the angular frequency of the normalized transverse wake with quality factor Q and $w(\zeta) = \Theta(\zeta)e^{-\zeta/(2Q)} \sin \zeta$, where $\Theta(\zeta)$ is the unit step function and the wake amplitude w_0 is embedded into the dimensionless coupling coefficient ϵ . The quadrupoles' focusing strength is represented by κ^2 and their transverse offset by x_Q , while x_A denotes the transverse misalignment of the cavity structures. The longitudinal beam profile $F(\zeta)$ is a summation of δ -functions for a train of point bunches.

2 PERFECTLY ALIGNED LINACS

Recently, Bohn and Ng [2] have been successful in solving the MBBU equation analytically with BNS damping incorporated. Consider a train of M point bunches each containing charge q with a separation τ in time. At entry into the

linac, the bunches all have the same offset x_0 and zero divergence. For a perfectly aligned linac and quadrupole system ($x_Q = x_A = 0$), the envelope of the *transient* displacement of the m -th bunch, $\Delta x_m(\sigma) = x_m(\sigma) - x_{ms}(\sigma)$ with $m = 0, \dots, M-1$ is derived, where x_{ms} is the *steady-state* displacement, the result of having the deflecting wake first seeded with an infinitely long bunch train immediately preceding the actual bunch train:

$$\left| \frac{\Delta x_m(\sigma)}{x_0} \right| \simeq \left[\frac{\gamma(0)}{\gamma(\sigma)} \right]^{\frac{1}{4}} \frac{\sqrt{\mathcal{E}} \exp[c(\eta)\mathcal{E} - m\omega_r\tau/(2Q)]}{4m\sqrt{2\pi} |\sin(\omega_r\tau/2)|} \times \begin{cases} |1 - \eta^2|^{-\frac{1}{4}} & \eta \text{ not near } 1 \\ \left[\frac{4\mathcal{E}}{3} \right]^{\frac{1}{6}} \frac{\Gamma(\frac{1}{3})}{\sqrt{2\pi}} & \eta = 1 \end{cases} \quad (2)$$

The auxiliary relations comprising Eq. (2) are:

$$\begin{aligned} \mathcal{E}(\sigma, m) &= \sqrt{\frac{mw_0eq\ell^2}{2\pi\nu_\beta\gamma(0)E_0}} \sqrt{\Sigma(\sigma)\Sigma(1)}, \\ \eta(\sigma, m) &= \frac{\pi\nu_\beta|f_\gamma|}{\mathcal{E}} \frac{m}{M} \frac{\Sigma(\sigma)}{\Sigma(1)}, \\ c(\eta) &= \begin{cases} \frac{\sqrt{1-\eta^2}}{2} + \frac{1}{4\eta} \tan^{-1} \left[\frac{2\eta\sqrt{1-\eta^2}}{1-2\eta^2} \right] & \eta < 1 \\ \frac{\pi}{4\eta} & \eta \geq 1, \end{cases} \\ \Sigma(\sigma) &= \int_0^\sigma d\sigma' \sqrt{\frac{\gamma(0)}{\gamma(\sigma')}} \xrightarrow[\text{acceleration}]{\text{uniform}} \frac{2 \left[\sqrt{\gamma(\sigma)/\gamma(0)} - 1 \right]}{\gamma(1)/\gamma(0) - 1}. \end{aligned}$$

in which e is the charge of the electron, ν_β denotes the betatron tune, i.e., the number of betatron wavelengths along the linac, and $\gamma(0)E_0/\gamma(1)E_0$ are the particle energies at the linac entrance/exit. The resonant effect of the transverse wake resides clearly in the denominator of Eq. (2), but the above solution is valid only far away from resonance. The total fractional energy spread across the bunch train, f_γ , or twice the total fractional focusing variation, is embedded in the parameter η .

In the derivation, the betatron tune ν_β is assumed to be much larger than both the perturbation of the wake and the relative acceleration gradient. This justifies the employment of the WKB approximation. The method of steepest descent has been used to arrive at the asymptotic behavior of the displacement envelope, and is valid provided the energy chirp is small and the bunch number m is sufficiently large. In order for the derivation to go through analytically, it has been assumed that the betatron tune decreases with energy as $\gamma(\sigma)^{-1/2}$, an arrangement closely resembling that of the SLAC proposed NLC. This deployment allows all the quadrupoles to be identical and their power driven by one common bus. Also assumed in the last auxiliary expression, although not necessary, is a linear acceleration profile in the linac.

We now apply the solution to designs of the SLAC NLC and DESY TESLA. Some parameters are listed in Table 1.

* Operated by the Universities Research Association, under contracts with the US Department of Energy.

Table 1: Some parameters of the SLAC NLC and DESY TESLA.

	NLC [†]	TESLA
Linac length ℓ (km)	10.0	14.4
No of betatron wavelengths ν_β	100	60
Entry/exit energy (GeV)	10/1000	5/250
No of bunches per train M	90	2820
Bunch charge q (nC)	-1.0	-1.6
Bunch spacing τ (ns)	2.8	377
Transverse wake:		
amplitude w_0 (V/pC/mm/m)	1	0.015
frequency $\omega_r/(2\pi)$ (GHz)	14.95	1.70
effective quality factor Q	∞	~ 125000

[†]The above belong to an older model of the SLAC NLC, and are chosen to illustrate MBBU. The parameters w_0 and Q represent a worst-case wake.

2.1 Amount of Energy Chirp

The transient displacements of the 90 bunches of the NLC at the linac exit were simulated and shown in Fig. 1 for energy spreads $f_\gamma = 1.5\%$ and 3.0% . It is clear that BNS damping is helping to control the emittance growth. The relative displacement of the 90-th bunch would be as large as 2.1 when $f_\gamma = 0$. We also see that with $f_\gamma = 3.0\%$ the envelope reaches a maximum at the 48-th bunch and decays algebraically afterward approaching steady state slowly. An effective BNS damping requires an energy spread sufficient to have the maximum to reach some bunches before they leave the linac. We learn by reviewing Eq. (2) that the envelope maximum corresponds to $\eta \gtrsim 1$, from which we obtain the criterion of required chirping as [2, 3]

$$|f_\gamma| \gtrsim \frac{\mathcal{E}(1, M-1)}{\pi\nu_\beta}, \quad (3)$$

which is plotted in Fig. 2 versus the wake amplitude for various strength of betatron focusing. For example, for the parameters in Table I, an energy chirp of $|f_\gamma| \gtrsim 2.18\%$ will be required. However, as will be seen in the next subsection, this is not the only criterion to control emittance growth.

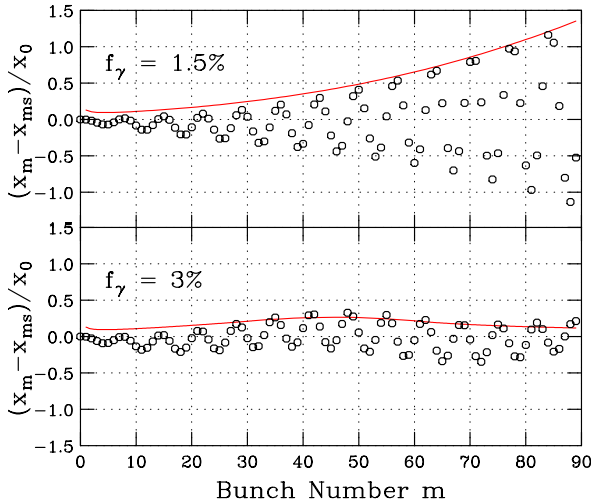


Figure 1: Analytic envelope of Eq. (2) at the linac exit (solid curve) of the SLAC NLC plotted against the simulated transverse bunch displacements, with total energy chirps of 1.5% (top) and 3.0% (bottom).

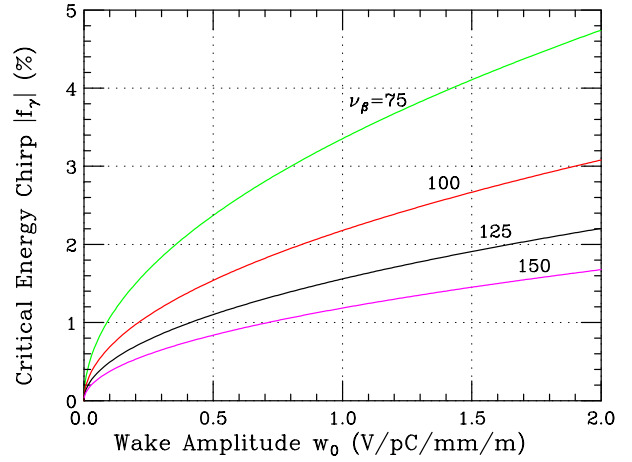


Figure 2: Critical energy chirp required for BNS damping in the SLAC NLC versus deflecting wake amplitude, with number of betatron wavelengths $\nu_\beta = 75, 100, 125$, and 150 .

2.2 The Quality Factor

Now let us apply the computed displacement envelope to the DESY TESLA. If the quality factor of the deflecting wake were infinite, Eq. (3) would require an energy chirp of $|f_\gamma| = 9.27\%$. This chirp is rather large because of the long bunch train of 2820 bunches. Even with such a large chirp, Eq. (2) predicts a normalized transient displacement envelope of $|\Delta x_m/x_0| = 296$ for the last bunch at the linac exit, and such emittance growth is totally unacceptable. Fortunately, the transverse long-range wake of the TESLA linac in Fig. 3 shows considerable amount of damping [4]. However, the wake does not correspond to a damped resonance of a single frequency. Assuming a resonant frequency of 1.7 GHz, one obtains a quality factor of $Q = 22400$ by comparing the wake envelope at the first and 10-th bunch spacings, $Q = 69000$ by comparing the wake envelope at the first and 100-th bunch spacings, and $Q = 124000$ by comparing the wake envelope at the first and 265-th bunch spacings (which is the end of the wake displayed in Fig. 3). In the discussion below, we set the quality factor as $Q = 125000$. Numerically, we find that $|\Delta x_m/x_0|$ never exceeds 0.012 and damps to less than 0.010 within the first 150 bunches, where no energy chirp has been applied (see top plot Fig. 10 below). It is important to mention that the theoretical pre-

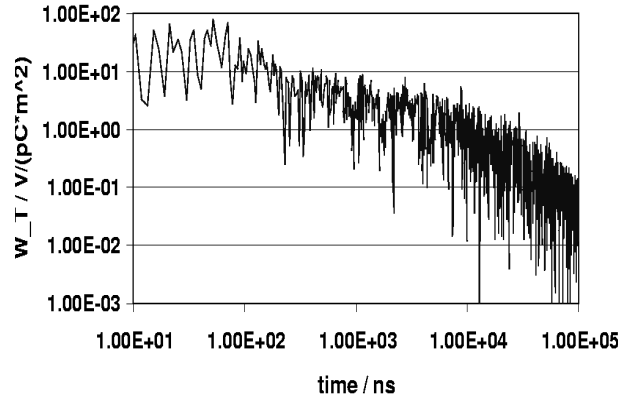


Figure 3: Plot of transverse long-range wake of the TESLA linac.

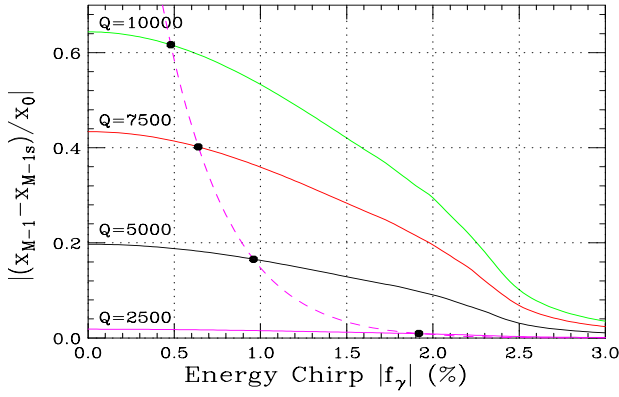


Figure 4: Plot of normalized transient displacement envelope of the last bunch at the linac exit of the SLAC NLC versus energy chirp $|f_\gamma|$ for various quality factors Q of the deflecting wake. The amount of equivalent energy-chirp-like damping provided by the finite quality factor is also shown as dashes.

diction of Eq. (2) may not apply to the TESLA linac, where MBBU is not severe because of the rather small effect from the transverse wake. Instead of the method of steepest descent, the MBBU equation should be solved by iteration with the coupling coefficient ϵ considered as a small quantity.

We can also visualize a finite quality factor Q of the deflecting wake as acting like an energy chirp. From the growth exponent of Eq. (2), it is evident that a finite quality factor will offset a certain amount of growth [3]. Setting $\eta = 1$ in the exponent, we obtain for the last bunch at the linac exit

$$|f_\gamma| = \frac{2M\omega_r\tau}{\pi^2 Q}, \quad (4)$$

which is the equivalent amount of energy-chirp-like damping provided by the quality factor. In Fig. 4, we plot the normalized envelope displacement of the last bunch at the exit of the SLAC NLC linac as a function of the energy chirp $|f_\gamma|$ for various values of the quality factor. The large dots are the equivalent energy-chirp-like damping provided by the quality factor. The dashed curve joining all the large dots depicts Eq. (4). Notice that the displacement is approximately independent of the energy chirp until the stated threshold is exceeded, after which the displacement drops off relatively fast with increasing $|f_\gamma|$. As an illustration, recall that for a wake with an infinite quality factor, $|f_\gamma| = 2.18\%$ is required for BNS damping. However, when the quality factor is lowered to $Q = 5000$, Fig. 4 indicates an equivalent energy chirp of 0.96% . Thus, only $|f_\gamma| = 2.18 - 0.96 = 1.22\%$ will now be required. This is demonstrated in Fig. 5, where we can see the maxima of the displacement envelopes reside at the last bunch at the linac exit in both situations. A smaller quality factor not only reduces the amount of energy chirp required for BNS damping; it also helps to reduce the transient transverse displacement along the bunch train from $|\Delta x_m/x_0| = 0.76$ to a very much smaller value of 0.15 . Thus, for the sake of controlling emittance growth and damping MBBU, it is beneficial to have lower quality factors for the deflecting modes.

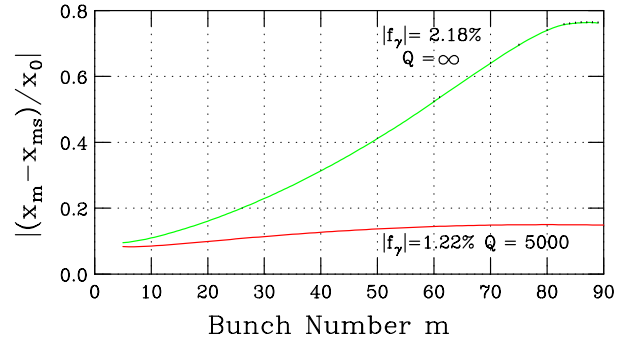


Figure 5: Plot of normalized transient displacement envelope at the linac exit of the SLAC NLC when envelope maximum occurs at the last bunch. Notice that the energy chirp $|f_\gamma|$ is reduced from 2.18% to 1.22% when the quality factor is reduced from $Q = \infty$ to 5000 .

Returning to the TESLA linac, Eq. (4) gives an “effective” energy chirp of $|f_\gamma| = 4600\%$ for the last bunch of the bunch train and 1.6% for the second bunch ($M = 1$). This explains why the transient displacement envelope was so heavily damped.

3 MISALIGNED LINACS

To arrive at an analytic solution, some assumptions are necessary. Consider the linac to be comprised of girders. On each girder is an accelerating length comprised of some number of rf structures and an optical element. Assume that the structures and quadrupoles are sufficiently well-aligned on the girders, leaving the girder misalignments as the dominating offset errors. If there are a large number of girders in each betatron wavelength, the beam will experience the same number of kicks due to the girder misalignments. Since the betatron wavelength is the characteristic *dynamic length*, the kicks act roughly as *white noise* on the beam. With these considerations, the quadrupole misalignment error $x_Q(\sigma)$ and structure misalignment error $x_A(\sigma)$ in Eq. (1) are the same random variable. In other words,

$$\langle x_{Q,A}(\sigma_1)x_{Q,A}(\sigma_2) \rangle = \frac{d_g^2}{N_g} \Sigma(\sigma) \delta(\sigma_1 - \sigma_2), \quad (5)$$

where N_g is the total number of girders in the linac and d_g is the rms girder misalignment. When the betatron focusing is strong, the MBBU equation can be solved in the same way as in Sec. 2. The result can be expressed analytically as

$$\frac{\langle \Delta x_m^e(\sigma)^2 \rangle^{1/2}}{\Delta x_m(\sigma)} \approx \frac{d_g}{x_0} \frac{2\pi\nu\beta}{\sqrt{N_g}} \begin{cases} \frac{1}{\sqrt{\mathcal{E}(\sigma, m)}} & \eta \leq 1 \\ \sqrt{\frac{2}{3}} & \eta > 1, \end{cases} \quad (6)$$

where $\Delta x_m^e(\sigma)$ is the transient displacement of the m -th bunch in the bunch train which enters the misaligned linac without any displacement errors, while $\Delta x_m(\sigma)$, given by Eq. (2), is the transient displacement of the m -th bunch in the bunch train which enters a perfectly aligned linac with initial displacement x_0 for all the bunches. The result is remarkable. First, it is simple. Second, it is independent of the amount of energy chirp f_γ either when $\eta \leq 1$ or $\eta > 1$.

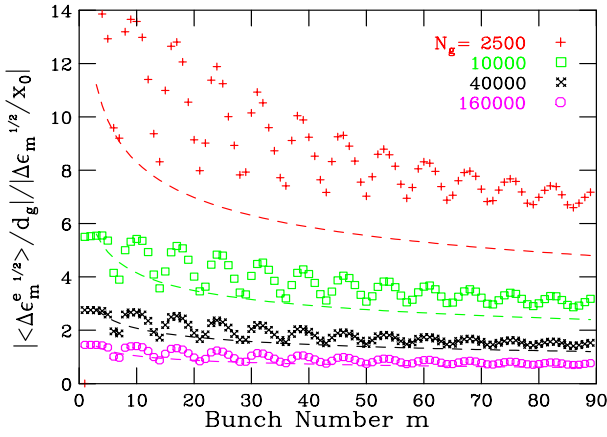


Figure 6: Plot of ratio of transient square-root-emittance with girder misalignments but no beam offsets to that with beam offset but no girder misalignments at the linac exit of the SLAC NLC. The results verify the $N_g^{-1/2}$ dependency of the theoretical predictions which are shown here in dashes. The energy chirp is 1.0%.

For $\eta = 0$, Eq. (6) reduces to Eq. (5.6) of Ref. [5], which was derived without any energy chirp. Also the derivation there was for square roots of the total emittances rather than the transient displacements.

3.1 Comparison with Simulations

In order to reduce the fluctuations due to betatron oscillation, we try to compute the transient square-root-emittance $\Delta \epsilon_m^e \frac{1}{2}$ instead of the transient displacement Δx_m^e , where the former is defined as*

$$\Delta \epsilon_m^e \frac{1}{2} = \left[(x_m^e)^2 + (\beta x_m^e)' \right]^{\frac{1}{2}} - \left[(x_{ms})^2 + (\beta x_{ms}')^2 \right]^{\frac{1}{2}}, \quad (7)$$

with β being the betatron function at the location along the linac under consideration and x_m^e the divergence of the particle bunch. The subscript s denotes steady state. Thus, the left side of Eq. (6) is replaced by $|\langle \Delta \epsilon_m^e(\sigma) \frac{1}{2} \rangle| / \Delta \epsilon_m(\sigma) \frac{1}{2}$.

We performed simulations of the SLAC NLC linac and computed beam quantities at its exit ($\sigma = 1$). In order to reduce the large spreads of the bunch displacements due to the randomness of the girder misalignments, each situation was simulated with 20 seeds and the results averaged. Figure 6 shows the simulated results when girder numbers $N_g = 2500, 10000, 40000$, and 160000 were used, while the energy chirp was kept at $f_\gamma = 1.0\%$ all the time. The plot actually verifies the $N_g^{-1/2}$ dependency stated in Eq. (6). The theoretical predictions are also shown in dashes with the understanding that η is always less than unity. We see that Eq. (6) agrees with the simulated results, although it tends to underestimate the results in general[†]. Actually, there will not be $N_g = 160000$ girders in the NLC linac. This number is created only for the purpose to check the theoretical prediction. With a linac length of $\ell = 10$ km and $\nu_\beta = 100$ beta-

*The emittance defined here when divided by the betatron function is the usual unnormalized emittance.

[†]The agreement of theoretical predictions with simulations would be as good as in Figs. 11 and 12 of Ref. [5] if we had plotted the simulation results of all seeds instead of just the averages and also with the vertical axis in a logarithmic scale.

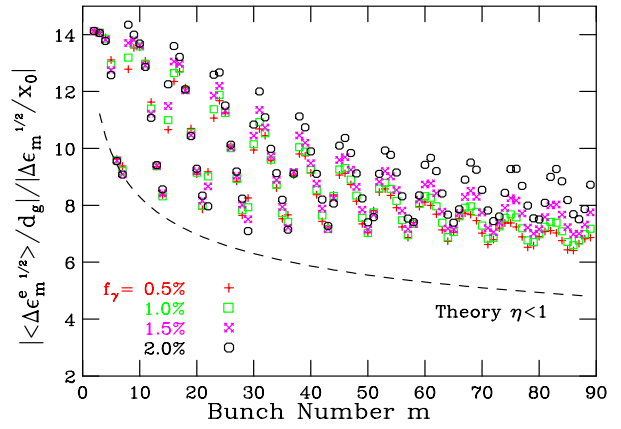


Figure 7: Plot of ratio of transient square-root-emittance with girder misalignments but no beam offsets to that with beam offsets but no girder misalignments at the linac exit of the SLAC NLC with energy chirp $f_\gamma = 0.5, 1.0, 1.5$, and 2.0% . The results appears to be f_γ -independent and follow the trend of the theoretical prediction for $\eta < 1$ shown here in dashes.

tron wavelengths, $N_g = 2500$ may be a reasonable number, which will be used in the discussions below.

Next we vary the energy chirp to $f_\gamma = 0.5\%, 1.0\%, 1.5\%$, and 2.0% . In all these cases, $\eta < 1$. We see in Fig. 7 that the simulation results fall on each other implying that there is no dependency on f_γ . Careful examination reveals that the ratio of the emittances appears to become larger for larger energy chirp especially when $f_\gamma = 2.0\%$. This is understandable, because the parameter η is closer to unity. The theoretical prediction is also shown; it appears to underestimate the simulation results.

Now let us examine the situation when $\eta > 1$. At the linac exit, η turns unity at the 48-th bunch when the energy chirp $|f_\gamma| = 3.0\%$, at the 18-th bunch when $|f_\gamma| = 5.0\%$, and at the 10-th bunch when $|f_\gamma| = 7.0\%$ [‡]. Simulations for these values of energy chirp are shown in Fig. 8. First, these results appear to be f_γ -independent. Second, the ratios of emittances are definitely larger than those in Fig. 7 where $\eta < 1$. Third, these results are mostly bunch-number-independent, unlike those in Fig. 7. These lead us to conclude that the results follow the theoretical prediction for $\eta > 1$.

3.2 Application

We learn from Figs. 7 and 8 that the ratios of the normalized transient square-root-emittances are, respectively, of the order 5 ($\eta < 1$) and 10 ($\eta > 1$) for the SLAC NLC linac, implying that the emittance growth from girder misalignments is much more serious than the growth from beam misalignment at linac entrance. In Fig. 9, we show the simulated normalized growth of transient square-root-emittance at the linac exit due to girder misalignment errors but without initial beam displacement errors. This growth is larger than the same growth of an initially displaced beam but without misalignment errors shown in Fig. 1. As a result, a larger energy chirp will be necessary to damp MBBU and control

[‡] $|f_\gamma| = 5$ and 7% would be unrealistically too high to survive the dispersive regions of the linear collider; $|f_\gamma| = 3\%$ is marginal.

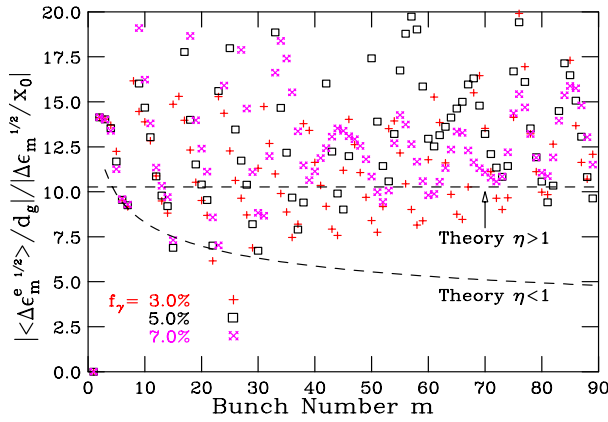


Figure 8: Plot of ratio of transient emittance with girder misalignment errors but no initial displacement errors to that with initial displacement errors but no misalignment errors at the linac exit of the SLAC NLC with energy chirp $f_\gamma = 3.0, 5.0,$ and 7.0% . The results appear to be f_γ -independent and follow the trend of the theoretical prediction for $\eta > 1$ shown in dashes.

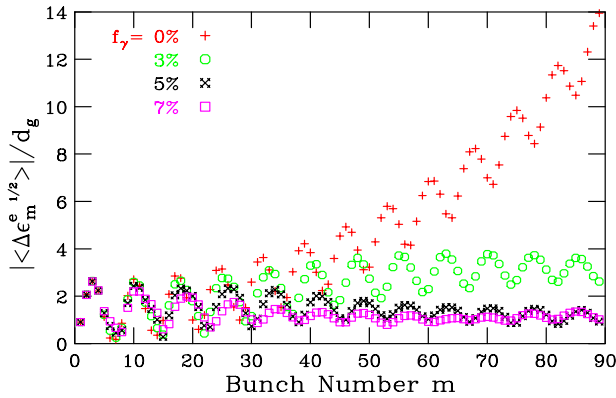


Figure 9: Plot of transient square-root-emittance with girder misalignments but no beam offsets at the linac exit of the SLAC NLC with energy chirp $f_\gamma = 0.0, 3.0, 5.0,$ and 7.0% . Compared with Fig. 1, larger energy chirp will be necessary for BNS damping.

emittance growth. We see that although the growth saturates at an energy chirp of $f_\gamma < 3\%$, the normalized growth has been 4-fold, and one needs an energy chirp of 5 to 7% to lower the growth to within 2-fold. On the other hand, for an initially displaced beam in a perfectly aligned linac, a 3% energy chirp controls the growth to less than 0.5 as indicated by Fig. 1.

Let us come back to the TESLA linac. Because of the small influence of the transverse wake, the displacements of the bunches possess rather good memory of their initial offsets when injected into the linac. As a result, in the absence of an energy chirp, the transient displacements, $\Delta x_m(\sigma)$, for all the bunches are more or less in phase during their betatron oscillations along the linac. The envelope of $\Delta x_m(\sigma)$ will become rather sensitive to the location of observation. To avoid ambiguity, the transient square-root-emittance, $\Delta \epsilon_m^{1/2}$, defined in Eq. (7) must be used. The top plot of Fig. 10 shows the simulated normalized transient square-root-emittance for a TESLA beam without energy chirp at the linac exit, where the linac elements are per-

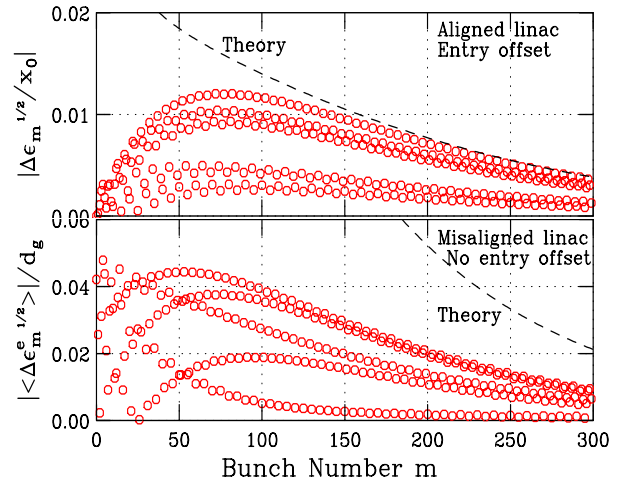


Figure 10: Simulated normalized transient square-root-

emittances for the first 300 TESLA bunches without energy chirp at the linac exit. Top plot is for bunches injected all with offset x_0 but no divergence in a perfectly aligned linac. Lower plot is for no injection offset, but the 2500 linac girders have rms misalignment d_g . Theoretical predictions are shown as dashes.

fectly aligned while the beam is injected with the same offset x_0 but no divergence for all the bunches. We see that with an effective quality factor of $Q = 125000$, the maximum normalized transient square-root-emittance is small and completely acceptable, around ~ 0.012 near the beginning of the bunch train and rolling off to ~ 0.005 near the 300-th bunch. The theoretical prediction [Eq. (2)] is shown as dashes, and unexpectedly agrees well with simulations for bunch number $m \gtrsim 150$. The lower plot shows the beam without offset at injection into the linac, but there are random misalignment errors in the 2500 girders. (Actually, each TESLA linac has less number of girders.) Although the normalized transient square-root-emittance becomes almost 4 times larger than the top plot, starting with the maximum of ~ 0.045 and rolling off to ~ 0.012 near the 300-th bunch, it is still acceptable. The theoretical prediction is shown as dashes and highly overestimates the simulation results. The disagreement is not hard to understand. Both Eqs. (6) and (1) do not apply well to the TESLA situation where the wake effect and MBBU are small. This prediction here is the product of the expressions in Eqs. (6) and (1) and therefore accumulates more uncertainty.

4 REFERENCES

- [1] V. Balakin, S. Novpkhatsky, and V. Smirnov, Proc. of 12th Int. Conf. on High Energy Accel., Fermilab, 1983, p.119.
- [2] C.L. Bohn and K.Y. Ng, "Preserving High Multibunch Luminosity in Linear Colliders", Phys. Rev. Lett. **85**, 984 (2000); *ibid*, 5010 (2000).
- [3] C.L. Bohn and K.Y. Ng, "Theory and Suppression of Multibunch Beam Breakup in Linear Colliders", Proc. of XX Int. Linac Conf., Aug. 21-25, 2000, Monterey, CA.
- [4] TESLA Technical Design Report, DESY Report 2001-011.
- [5] K. Yokoya, "Cumulative Beam Breakup in Large-scale Linacs", DESY Report 86-084, 1986.